

2. BACKGROUND FATIGUE THEORY

The aim of this chapter is to establish the basis for other chapters : not only to outline the scope of the study and review the subjects belonging within the scope, but also to analyze the relationships between reviewed subjects.

Three main subjects under consideration will be : *stress concentrators* - in order to understand *where* fatigue occurs ; *fatigue crack propagation* - in order to understand *how* fatigue occurs ; and *fatigue life prediction methods* - in order to review existing approaches destined to analyze *when* fatigue occurs. A brief introduction which includes the definition of fatigue as well as a short historical background precedes the review of other subjects.

2.1 INTRODUCTION

The word *fatigue* comes from the Latin verb *fatigare* - "to tire". There are many ways to define *engineering fatigue* (Radaj [2.1], Gurney [2.2], Lemaitre [2.3]). Below, two of them, are given :

- definition evoking *technical* aspects of the word 'fatigue' is : fatigue is a term, which applies to changes in properties which can occur in a metallic material due to the repeated application of stresses and strains, although usually this term applies specially to those changes which lead to cracking and failure , [2.4] ;
- definition related to the word '*engineering*' is : fatigue shows the inability of an engineer to design structures that support relatively small cyclic loads for a long time .

There has been research in the area of fatigue : Some of the earliest research was conducted during the first half of the nineteenth century. Some milestones during the development of fatigue science are well worth noting and are listed herein (a complete list of historical events can be found in [2.5]) :

- 1829** Albert, the German mining engineer, performed the first probable study of metal fatigue [2.6]. He rendered repeated load proof tests on mine-hoist chains made of iron.
- 1839** Poncelet introduced the term *fatigue* in connection with metal failure.
- 1843** W. J. M. Rankine, a British railway engineer, recognized the distinctive characteristics of fatigue fractures and noted the dangers of stress concentrations in machine components.
- 1860** Wöhler conducted systematic investigations of fatigue failure in railroad axles for the German Railway Industry. He observed that the strength of the steel axles subjected to cyclic loads was much lower than the static strength. His work also led to the characterization of fatigue behavior using stress amplitude-life (*S-N*) curves and the concept of the fatigue 'endurance limit'.
- 1910** Basquin proposed empirical laws to characterize the fatigue endurance limit of materials.
- 1913** Inglis, by using stress analyses, and **1921** Griffith, by using an energy concept, provided the mathematical tools for quantitative treatments of fracture in brittle solids.
- 1924** Palmgren developed a damage accumulation model for fatigue failure.
- 1939** Westergaard developed a method to determine the stress and displacement field ahead of the sharp crack tip.
- 1945** Miner developed a damage accumulation model for fatigue failure.

- 1954** Coffin and Manson discovered independently that plastic strains are responsible for cyclic damage. They proposed an empirical relationship between the number of load reversals to fatigue failure and the plastic strain amplitude.
- 1957** Irwin showed that the amplitude of the stress singularity ahead of the crack could be expressed in terms of a scalar quantity known as the stress intensity factor (K).
- 1960** Dugdale [2.7] and **1962** Barrenblatt [2.8] introduced simple crack models.
- 1961** Paris, Gomez and Anderson were the first to suggest that fatigue crack propagation rate per stress cycle, da/dN , could be related to the range of the stress intensity factor, ΔK .
- 1970** Elber showed that fatigue cracks could remain closed even when subjected to cyclic tensile loads. His work created a base for development of the crack-closure concept.

Fatigue can be classified by the form in which it occurs : mechanical, creep, thermo-mechanical, corrosion, rolling contact, and fretting fatigue (Suresh [2.5]). Fatigue can also be classified by the duration of the fatigue life : low-cycle and high-cycle fatigue. This study only examines *mechanical* and *high-cycle* fatigue - the most common fatigue types in civil engineering.

A fatigue crack can propagate in three modes, depending on the relative orientation of loading to the crack (Figure 2.1). This study focuses on mode I crack growth - the most common crack propagation mode.

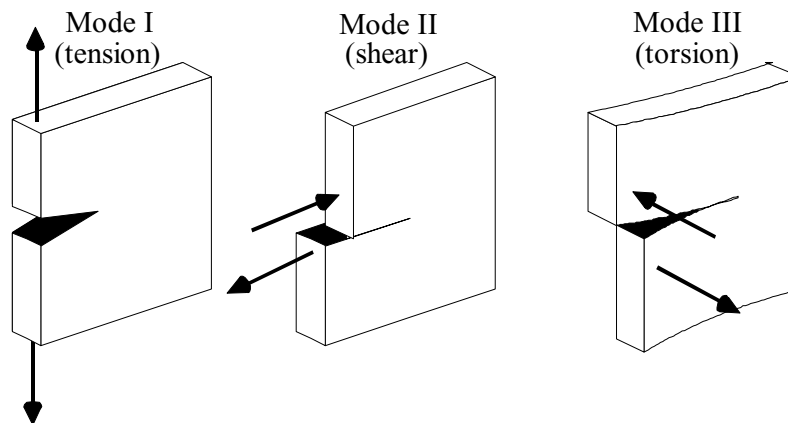


Figure 2.1 : Crack propagation modes.

2.2 STRESS CONCENTRATORS

Complex *structural details* contain regions where there are changes in geometry. These regions are called *stress concentrators* (Figure 2.2). Local stress fields near stress concentrators are considerably larger than nominal stress away from the stress concentrators.

Fatigue cracks typically appear near the stress concentrators. The stress concentrators, leading to the appearance of fatigue cracking, can be called *crack initiators*. Crack initiators can be holes, welds, notches, or regions where material structure changes. The fatigue crack itself is also a stress concentrator because a very intense stress field is present around the crack tip. In this study, the stress concentrators are classified into two groups : *crack initiators* and *fatigue cracks*.

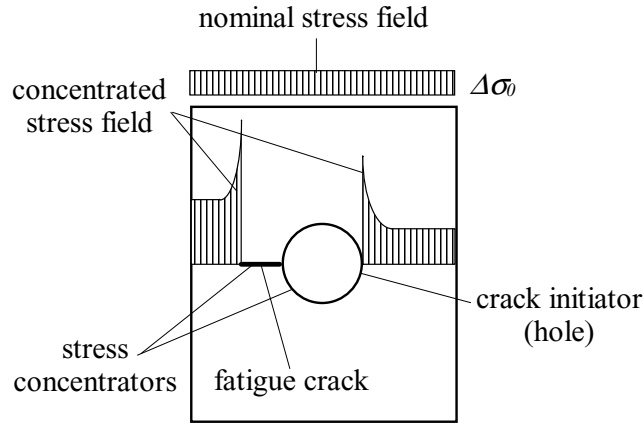


Figure 2.2 : *Stress concentrators.*

The influence of the stress concentrators on fatigue behavior can be characterized by the linear-elastic stress field generated around the stress concentrator. Calculation of the linear-elastic stress field depends on the geometry of the stress concentrator. The geometry of the crack initiators usually differs from the geometry of the fatigue cracks; therefore, the calculation of the linear-elastic stress field around the crack initiators will be discussed separately of the calculation of the linear-elastic stress field around the fatigue crack.

Structural details usually contain residual stresses introduced during the fabrication process. These residual stresses also influence the stress field around the stress concentrators and must be considered. Further in this section, a calculation of the linear-elastic stress field around the stress concentrators, without and with considering residual stresses, is presented.

2.2.1 Crack Initiators

Linear-Elastic Stress Field

The linear-elastic stress field around the crack initiator can be expressed through the *stress concentration factor (SCF)*. The stress concentration factor at any point of the detail is the ratio of the local linear-elastic stress component at this point to the corresponding nominal stress component (Figure 2.3). Taking the x coordinate along the crack path, the stress concentration factor can be calculated at any value of x , using Equation (2.1) :

$$SCF(x) = \frac{\sigma_{le}(x)}{\sigma_0} \quad (2.1)$$

where $\sigma_{le}(x)$ is the local linear-elastic stress acting perpendicularly to the x -axis¹. The stress concentration factor distribution along the net section of the plate with a hole in the center is presented in Figure 2.3. Stress concentration factor distributions are given for two values of hole diameter, d , and are calculated using an analytical solution from [2.9].

¹ In cases in which the crack path is not a straight line, the direction of the $\sigma_{le}(x)$, then changes with the change of the crack's path direction.

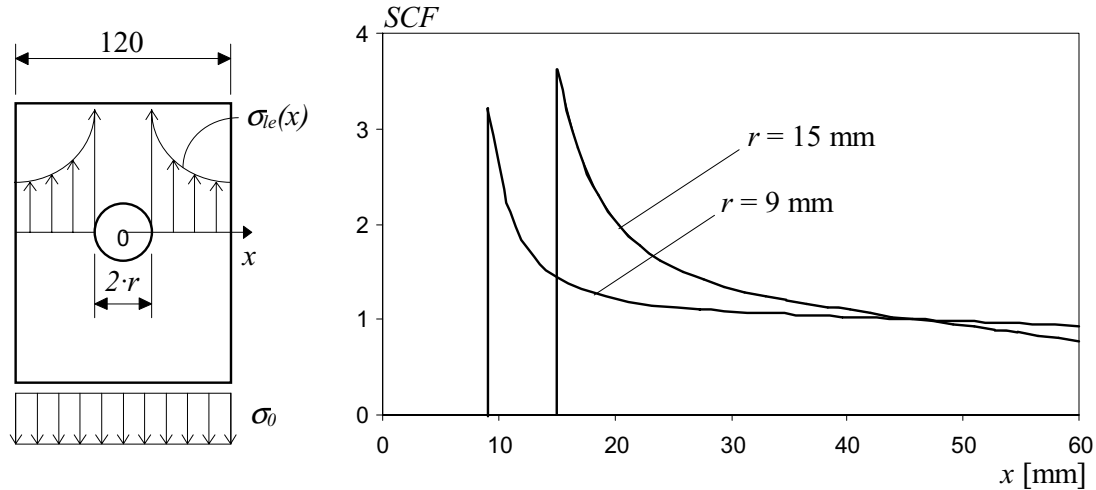


Figure 2.3 : The stress concentration factor for a plate with a hole in the center.

The local linear-elastic stress, $\sigma_{le}(x)$, in Equation (2.1), can be calculated using numerical methods (linear-elastic finite-element analysis of the detail, analytical determination¹) or experimental methods (measuring with strain gauges, photoelasticity method [2.14]). The most widely used way to calculate the stress concentration factor is *finite element method*. The advantage of this method is that it permits the stress concentration factors for details with very complicated geometry to be determined.

Residual Stresses

The influence of fabrication-introduced residual stresses on the linear-elastic stress field can also be expressed using the stress concentration factor :

$$SCF(x) = \frac{\sigma_{le}(x) + \sigma_{res}(x)}{\sigma_0} \quad (2.2)$$

where $\sigma_{res}(x)$ is the residual stress at the x coordinate acting perpendicular to the crack path². The stress concentration factor $SCF(x)$ in Equation (2.2) is a function of detail geometry *and* residual stress.

2.2.2 Fatigue Cracks

Linear-Elastic Stress Field

The linear-elastic stress field at the tip of a sharp crack (or at the tip of a sharp notch) can be calculated using a *stress intensity factor*³ (K_I). There are many methods to compute the linear-elastic stress field at a sharp crack tip [2.10], [2.11], [2.12], [2.13]. The complete stress field can be expressed by the Equation (2.3) :

¹ Analytical stress concentration factor solutions exist for plates containing holes, see [2.9].

² The $SCF(x)$ in Equation (2.2), is a function of the detail geometry and fabrication-induced residual stress, while $SCF(x)$ in Equation (2.1), is a function of the detail geometry only.

³ The inverse formulation is also true : if the intensity (the distribution) of the linear-elastic stress field around the crack tip is known, then the stress intensity factor for a given crack size and type can be calculated.

$$\sigma_{i,j} = \frac{K_I}{\sqrt{2 \cdot \pi \cdot r}} \cdot f_{i,j}(\theta) + 2^{\text{nd}} \text{ term} + 3^{\text{rd}} \text{ term} + \dots + n^{\text{th}} \text{ term} \quad (2.3)$$

where $\sigma_{i,j}$ are the stresses acting on a material element $dx \cdot dy$ at a distance r from the crack tip and an angle θ from the crack plane. The stress intensity factor, K_I , corresponding to the mode I cracking (later on K will be used instead of K_I), and $f_{i,j}(\theta)$ are geometrical functions of θ (Figure 2.4). For values of small r , the first term in Equation (2.3) is much greater than the following terms, and it is often sufficient to consider only the first term of Equation (2.3) very near the crack tip.

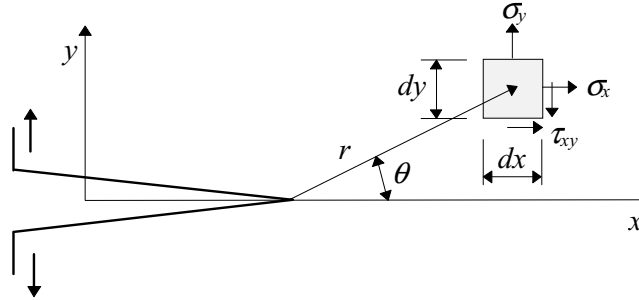


Figure 2.4 : Crack in arbitrary body.

Functions $f_{i,j}(\theta)$ can be found in the literature [2.12]. Since regarding mode I crack propagation θ can be taken 0. Since at the vicinity of crack tip, the stress field is mostly influenced by the first term of Equation (2.3), it is not necessary to consider the other terms of the equation. Herein, only the solution of the stress component σ_y at the plane $\theta = 0$ and the first term of Equation (2.3) is shown :

for an ideally *sharp* crack (Figure 2.5.a) :

$$\sigma_y = \frac{K}{\sqrt{2 \cdot \pi \cdot r}} \quad (2.4)$$

for *blunted* crack with tip radius ρ (Figure 2.5.b)¹ :

$$\sigma_y = \frac{K}{\sqrt{2 \cdot \pi \cdot r}} \cdot \left(\frac{\rho}{2 \cdot r} + 1 \right) \quad (2.5)$$

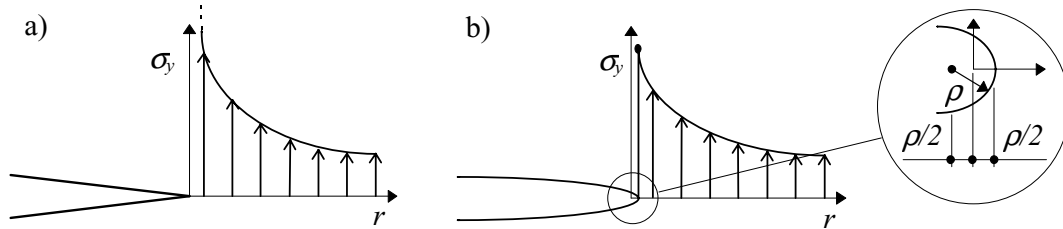


Figure 2.5 : Linear-elastic stress σ_y at the crack tip : a) sharp crack ; b) blunted crack with tip radius ρ .

¹ Equation (2.5) becomes Equation (2.4) if $\rho \ll 0$. Equation (2.4) has a singularity at the crack tip. By considering the co-ordinate system as indicated in Figure 2.5.b, the singularity at the crack tip disappears if Equation (2.5) is used.

Stress intensity can be considered as a similitude parameter. If the stress intensity factors of two non-similar cracks are equal, then the behavior of these cracks will be similar¹ (Broek [2.14]). The advantage of the stress intensity factor concept is that it is universal, i.e., the same calculation principles apply to the analysis of a great variety of fatigue cracks.

The stress intensity factor for a crack in an infinite 2-dimensional plate can be calculated using Equation (2.6) which was first given by Griffith [2.15].

$$K = \sigma_0 \cdot \sqrt{\pi \cdot a} \quad (2.6)$$

A more general formula for the stress intensity factor is :

$$K = Y \cdot \sigma_0 \cdot \sqrt{\pi \cdot a} \quad (2.7)$$

where Y is called *stress intensity correction factor*. The stress intensity correction factor is introduced to *normalize* the stress intensity factors for various cracks geometry and detail geometry, using the K -solution of the crack in the infinite 2-dimensional plate where the stress intensity correction factor is 1. The stress intensity correction factor Y for a center-cracked plate with a hole is presented in Figure 2.6. Determination methods of the stress intensity correction factors are given in appendix A.1.

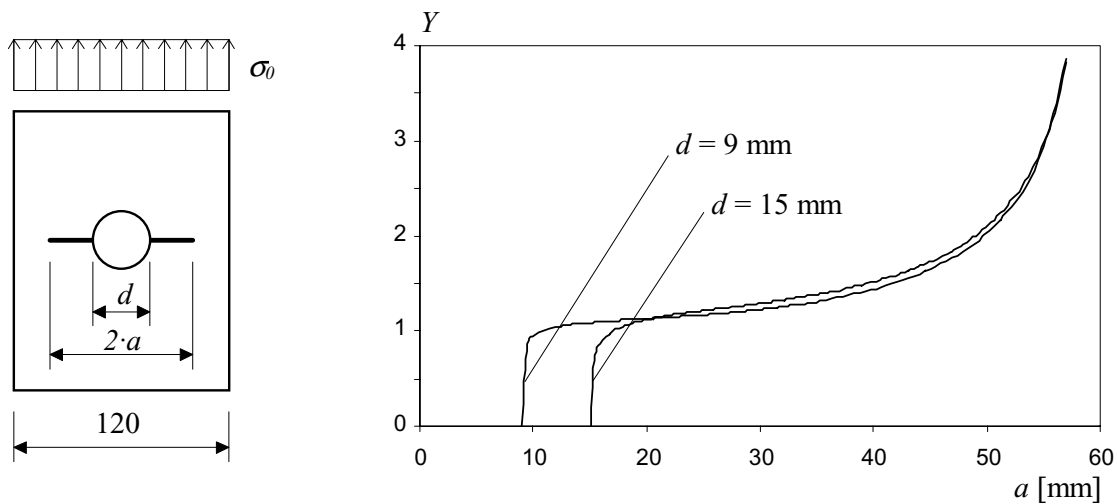


Figure 2.6 : Stress intensity correction factor for a center-cracked plate with a center hole [2.18].

Residual Stresses

Fabrication-introduced residual stresses can also be accounted for by the stress intensity factor. The stress intensity factor due to fabrication-introduced residual stress, K_{res} , can be evaluated using a method proposed by Albrecht and Yamada [2.16].

$$K_{res} = F_f \cdot \sqrt{\frac{a}{\pi}} \cdot 2 \cdot \int_0^a \frac{\sigma_{res}(x)}{\sqrt{a^2 - x^2}} \cdot dx \quad (2.8)$$

¹ The stress intensity factor is not the only similitude parameter of fatigue cracks : the plastic zones of compared cracks should also be approximately of same size.

Factor F_f in Equation (2.8) takes into account crack geometry and can be obtained in several handbooks [2.17], [2.18], [2.19] (see also appendix A.1). The overall stress intensity factor, K_{tot} , is the sum of the stress intensity factors due to the nominal load and residual stress :

$$K_{tot} = K(\sigma_0) + K_{res} \quad (2.9)$$

2.3 FATIGUE CRACK PROPAGATION

If the structural detail is loaded cyclically, very small cracks, or micro-cracks, appear at the crack initiators. Those micro-cracks can join together and result in a *fatigue crack*. This procedure is called *crack¹ initiation*. The initiation *and* growth of the fatigue crack under cyclic loading is called *fatigue crack propagation*.

2.3.1 Crack Propagation Stages

Fatigue crack propagation can be divided into three *stages* as shown in Figure 2.7 : crack initiation (CI), stable crack growth (SCG), and unstable crack growth (UCG).

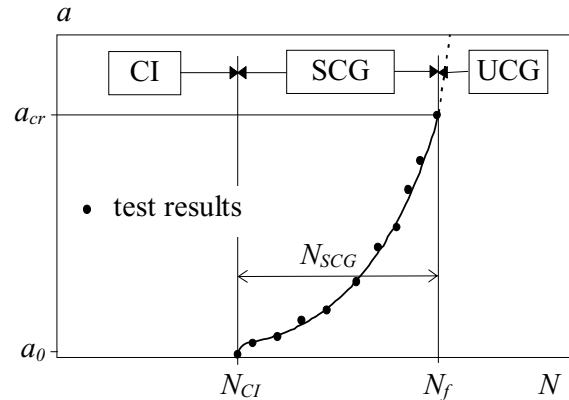


Figure 2.7 : Fatigue crack propagation stages.

Crack Initiation

Crack initiation takes place at the crack initiators. The length of the initial crack is marked as a_0 and it is usually taken between 0.1 to 0.25 mm [2.20], [2.21]. The number of stress cycles corresponding to crack length a_0 in the a - N curve is referred to as the *crack initiation life* and it is noted N_{CI} (Figure 2.7).

The crack initiation life can be *absolute* and *relative*. The *absolute* crack initiation life depends on the *magnitude* of the local cyclic stress field around the stress concentrator. The *relative* crack initiation life (compared to the total fatigue life of the specimen) depends on the *distribution* of the local cyclic stress field around the stress concentrator².

¹ From now on, the shorter word ‘crack’ will sometimes be used instead of ‘fatigue crack’.

² The crack initiation life of a smooth low-cycle fatigue test specimen, for example, constitutes the major portion of the total fatigue life : $N_{CI} \cong 0.9 \cdot N_f$. This is because the stress distribution along the critical section is uniform. Unlike the smooth low-cycle fatigue test specimens, the crack initiation life of *welded* details only constitutes a small part of the detail’s total fatigue life : $N_{CI} \cong 0.1 \dots 0.3 N_f$. This is because very high local stress concentrations are present in the material close to the weld toe. These high stress concentrations rapidly decrease beyond the weld toe.

Stable Crack Growth

Stable crack growth takes place along a path perpendicular to the dominant principal stress. The number of load cycles required to grow the crack from its initial length a_0 , to the critical length a_{cr} , is called the stable crack growth life and it is given the symbol N_{SCG} . The total fatigue life, N_f , is the sum of the N_{CI} and N_{SCG} (Figure 2.7)¹.

Similar to the crack initiation stage, an *absolute* and *relative* stable crack growth lives can be defined. The *absolute* stable crack growth life is primarily influenced by the *magnitude* of the nominal stress range. The *relative* stable crack growth life depends on the *distribution* of the local cyclic stress field along the crack propagation path.

Figure 2.8 illustrates the influence of the stress distribution along the crack path on the *relative* crack initiation and stable crack growth lives. The plates in Figure 2.8 contain an elliptical hole at the center. In case a), there is a relatively uniform stress distribution along the crack path which results in a *long* relative crack initiation life (Figure 2.8.a). However, in case b), the non-uniform, rapidly decreasing stress distribution along the crack path results in a *short* relative crack initiation life (Figure 2.8.b).

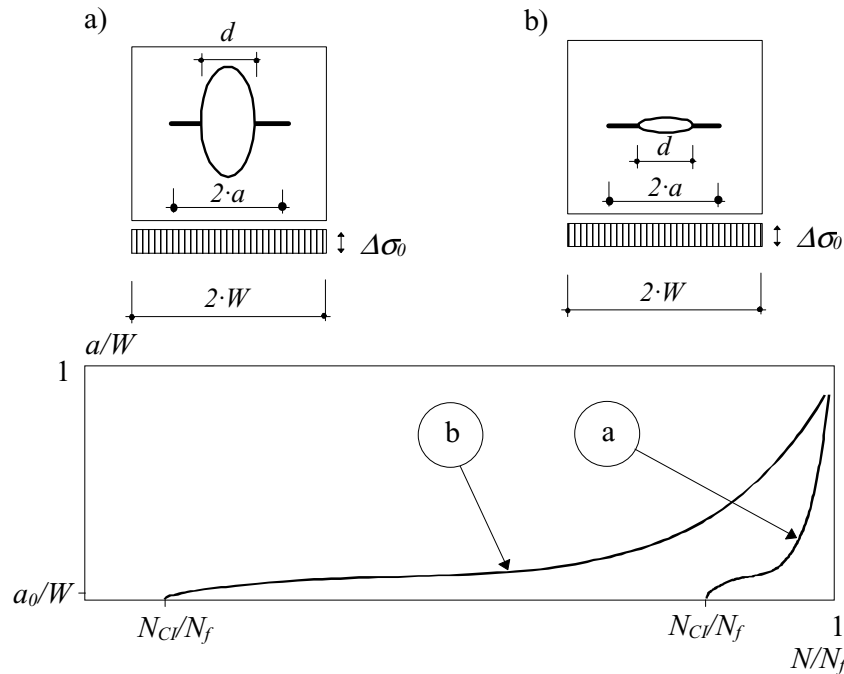


Figure 2.8 : Relative crack initiation life as a function of the stress distribution at the crack initiator : a) $N_{CI} \gg N_{SCG}$; b) $N_{CI} \ll N_{SCG}$.

Unstable Crack Growth

If crack propagation has entered into the unstable growth stage, a ductile or brittle fracture of the detail can take place. This phase of the fatigue crack propagation is very short compared to the crack initiation and the stable crack growth phases. Since the unstable crack growth stage

¹ Here the total fatigue life does not correspond exactly to the number of load cycles until the failure of the detail. However, the unstable crack growth life is very short compared to the total fatigue life, and in this study it is assumed that N_f approximately corresponds to the load cycles until the failure.

is only a small part of the total fatigue life, it is not important from a practical point of view. Therefore, modeling of the unstable crack growth stage will not be discussed further.

2.3.2 Fatigue Crack Advance

Fatigue crack advance can be defined as a change in the crack tip coordinate. There are two different types of crack advances: advance which occurs *after several* load cycles and advance occurring *at every* load cycle. The aim of this section is to determine when the change in crack advance type occurs. Distinguishing between crack advance types is important from the point of view of modeling, because it is assumed that the two types of crack advance must be modeled in different ways.

Crack Advance after Several Load Cycles

In this case, fatigue crack growth is the result of *micro-crack nucleation and propagation*. A fatigue crack advances when micro-cracks close to crack tip join together. Micro-crack nucleation takes place at the material grain scale level. It occurs at surface roughness occurring as the result of an irreversible shear slip on different glide planes (Wood [2.22]); at grain boundaries (Kim and Laird [2.23]); at micro-structural defects, such as pores and inclusions (Bowles and Schijve [2.24]); and at corrosion pits. Nucleated micro-cracks propagate, join together, and form a fatigue crack, or cause crack advance if latter has already been formed.

Crack Advance at Every Load Cycle

In this case, a fatigue crack advances as the result of *local fracture* of the material, which occurs in *every* load cycle. Local fractures can have a brittle character (cleavage fracture) or ductile character (ductile fracture). Fracture surfaces form *fatigue striations*. These striations were first observed by Zappfe and Worden [2.25]. The fatigue striations appear as ripples on the fracture surface. Not all engineering materials form fatigue striations; however, they are clearly seen in pure metals and in many ductile alloys.

Crack Advance Types versus Crack Propagation Stages

If a fatigue crack advances at every load cycle, then the fatigue striations appear at the cracked surface. Fatigue striations are indicators of the change in the type of crack advance. Broek and Leis [2.26] reveal that the smallest observed striation spacing is greater than 10^{-5} mm. Published photos show, however, the formation of striations only when the crack propagation rate da/dN is about 10^{-4} to 10^{-3} mm/cycle ([2.27]). This implies that the crack advance at every cycles takes place only *at the end* of the stable crack growth stage and during the unstable crack growth stage¹.

It can be concluded that during the most portion of the total fatigue life, each fatigue crack advance occurs after several load cycles. And only at the end of the stable crack growth stage and during the unstable crack growth stage, a fatigue crack advances *at every* load cycle. This is graphically presented in Figure 2.9.

¹ Suresh [2.5] says that fatigue striations already occur in the beginning of the stable crack growth stage ($da/dN \sim 10^{-6}$ mm/cycle), and Ritchie [2.1] states, that the striation related growth dominates when $da/dN \sim 10^{-6}$ to 10^{-4} mm/cycle. It seems that there is a contradiction between the statements of Suresh and Ritchie, and the published photos about fatigue striations.

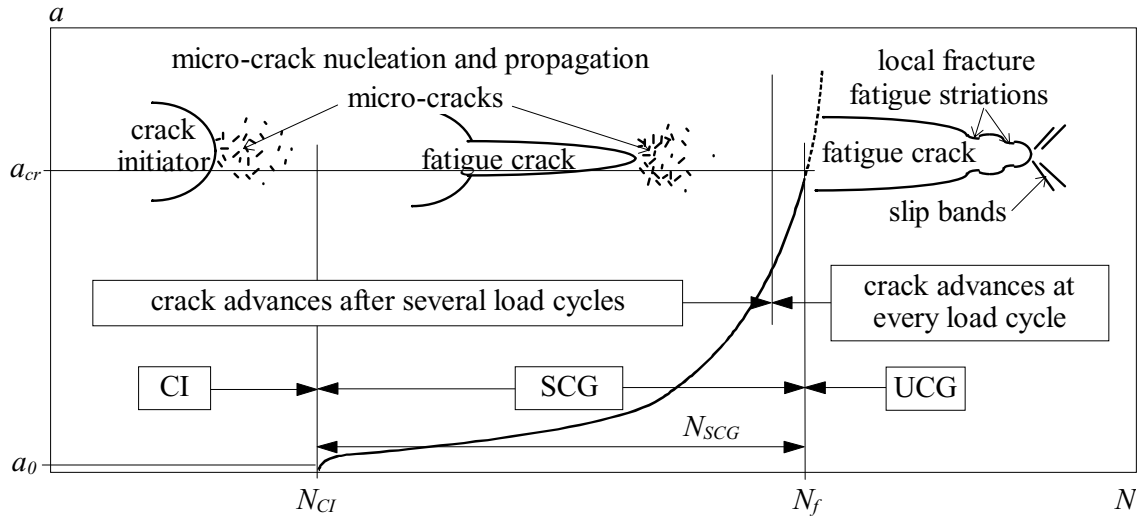


Figure 2.9 : Crack propagation mechanisms compared to the crack propagation stages.

2.3.3 Selected Aspects of Fatigue Crack Propagation

Observations made on cyclically loaded fatigue test specimens and structures show that a number of specific aspects related to the fatigue crack propagation exist. A general and reliable fatigue model must be able to simulate these aspects. In this section, the most important of these aspects are discussed.

Fatigue Threshold

If very low cyclic stresses are applied on a *non-cracked* detail, fatigue cracks will not initiate. If very low cyclic stresses are applied on *cracked* detail, the crack propagation will stop. A non-initiation or non-propagation of fatigue crack means that the material around the crack initiator or fatigue crack is not (any more) cyclically damaged. The nominal stress level at which the cyclic damage evolution stops is called *fatigue threshold*.

A physical explanation of the fatigue threshold is that if nominal load ranges are very small, then local cyclic strains around the stress concentrator, do not exceed the elastic range. This means that no plastic deformation (dislocation movement) occurs around the grain scale stress concentrators, micro-cracks do not nucleate, and local damaging of material does not develop. Due to the practical importance of the fatigue threshold, fatigue crack propagation models *must* be able to simulate this aspect.

Crack Closure Effect

Before explaining the *crack closure effect*, the components of the fatigue crack are presented. When loading a cracked detail, very high stress concentration fields develop around the crack tip. The material cannot support these high stresses and attempts to redistribute the stress field, corresponding with the strain's increase. Due to the increase in strain, the material will yield and a *plastic zone* will form around the crack tip. The crack edge is surrounded with a strip of plastically deformed material, referred to as the *plastic strip*. This plastic strip is created when the crack advances. A typical fatigue crack with these two components, plastic zone and plastic strip, is illustrated in Figure 2.10.

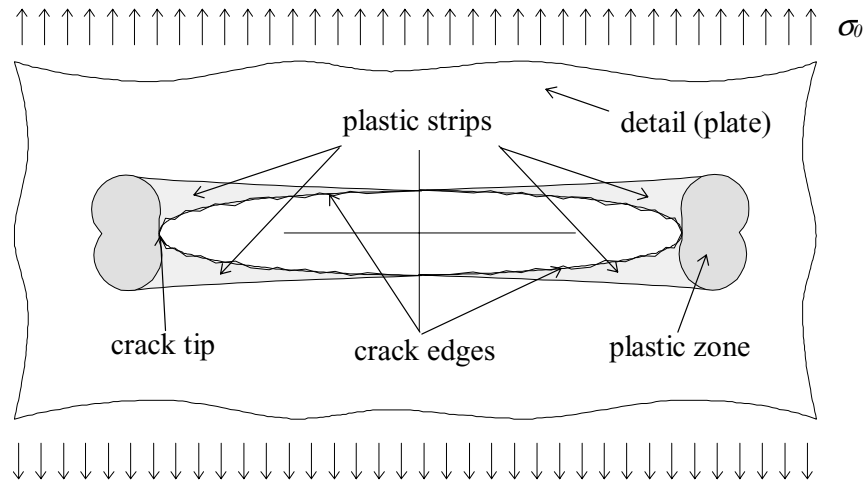


Figure 2.10 : A fatigue crack and its components.

The crack closure effect was first discovered by Elber [2.28], [2.29]. Elber argued that the zone of residual tensile deformation (plastic strip) is left in the wake of a fatigue crack tip. The corresponding reduction in crack opening displacement (reduction occurs due to plastic strip) gives rise to premature contact between the faces of the crack edges on unloading and causes a reduction in the cyclic deformations around the crack tip. The reduction of the cyclic deformations results in slower local damaging of the material at the crack tip and leads to a slower crack propagation. In summary, the premature closure of the crack (the crack closure effect) leads to a retardation of the fatigue crack propagation.

Suresh has identified several mechanisms of crack closure ([2.5]). This study considers only the *plasticity-induced* (premature closure of crack occurs due to the *plastic strip*) and *phase transformation-induced* crack closure (premature closure of crack occurs due to changes of the stress-strain state at the crack tip and corresponding change in volume of the crack tip *plastic zone*). These two crack closure mechanisms can be regarded as the main factors influencing fatigue damage resulting from the variable-amplitude load. Therefore, they must be taken into account when attempting to model fatigue behavior under *variable-amplitude* loading.

Variable-Amplitude Load Effects

The effects of variable-amplitude load on fatigue behavior result from the crack closure effect [2.30]. The four main categories of variable-amplitude load effects are as follows :

Mean stress effect. If two identical details are subjected to the same nominal stress range, but of a different nominal mean stress, then both crack initiation and stable crack growth occurs faster in the detail submitted to higher nominal mean stress [2.5], [2.14]. The increase in crack propagation velocity with increase of the mean stress is due to the simultaneous increase in maximum nominal stress and the increase in the volume of the crack tip's plastic zone. A larger plastic zone does not permit the premature contact of the crack surfaces and consequently the cyclic deformations at the crack tip increase. Thus, growth of the crack is accelerated.

Effect of tensile overload. Tensile overloads usually cause a short acceleration, followed by a long delay in crack growth [2.30] (Figure 2.11). An overload causes an increase in the crack plastic zone and prevents the premature contact of the crack surfaces just after the overload. Consequently, the cyclic deformations at the crack tip increase and the growth of the crack is accelerated. When the crack tip passes through the plastic zone created by the overload, a wide plastic strip remains in the wake of the crack tip. A widened plastic strip leads to the

premature contact of the crack surface. Consequently, the cyclic deformations at the crack tip decrease and the growth of the crack is slowed.

Effect of compressive overload. Single compressive overloads do not usually cause a change in the rate of crack growth. However, some studies [2.31], [2.32] have shown that compressive overloads can lead to an acceleration of crack growth (Figure 2.11). This phenomenon can be explained by the following. Compressive overloads, depending on their magnitude, can decrease the height of the plastic strip as well as the volume of the plastic zone. This prevents contact between the crack surfaces which would have occurred before applying the under-load. Future contact of the crack surfaces results in greater cyclic deformation at the crack tip, faster local damaging of the material, and accelerated crack propagation.

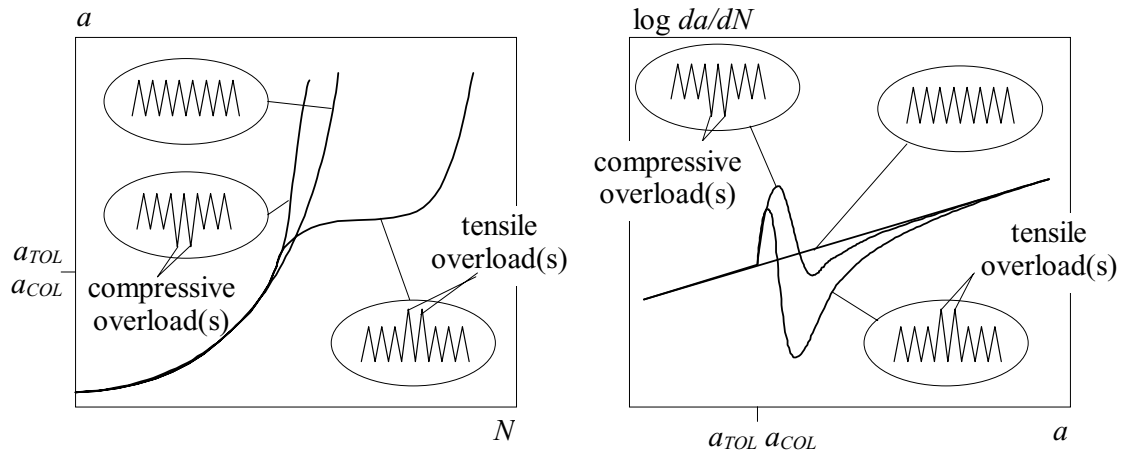


Figure 2.11 : Effect of tensile and compressive overloads on fatigue crack propagation.

Mixed load effects. The mixed load effects depend on the order in which the loads are applied. For example, a tensile overload preceding a compressive overload significantly reduces the delaying effect of the overload. However, if the compressive overload is applied before the tensile overload, then the rate of crack propagation decreases as if only the tensile overload had been applied [2.33].

All variable-amplitude crack propagation can be regarded as perpetual delaying and acceleration of crack growth, where the latter is a function of the nominal loading history. Due to the complexity of the field, it is impossible to analyze the effects of variable-amplitude loading separately from the crack closure effect. Therefore, the effects of crack closure must be considered in order to successfully model variable-amplitude fatigue behavior.

Other Aspects

Small crack behavior. It has been observed that small fatigue cracks grow much *faster* than predicted using linear elastic fracture mechanics (LEFM). Agreement between measured and predicted crack propagation rate is obtained only when the crack has become long enough. The phenomenon is so important that a considerable amount of research work has been carried out in this area [2.34].

Small crack behavior is usually explained by the crack closure concept. A more physical explanation of the small crack behavior can also be given; using linear elastic fracture mechanics does not take into account the damage in the region around the crack initiator caused during the crack initiation (Figure 2.12). At the beginning of the stable crack growth, the material around the crack tip has already been weakened by micro-cracks. These micro-cracks were introduced during crack initiation. The crack propagation at the beginning of the

stable crack growth stage is faster than predicted with LEFM because the latter assumes that the material around the initial crack tip has not been damaged. When the crack tip grows out of the initially damaged region, the rate of propagation slows down and attains the LEFM-predicted crack propagation rate.

The main reason why LEFM under-estimates the propagation rate of small cracks appears to be because of the influence of the initially damaged material is not conveyed on the growth of the short crack. Taking into account the initial damaging of the region ahead the tip of the small crack would improve the accuracy of modeling of the small crack behavior using LEFM.

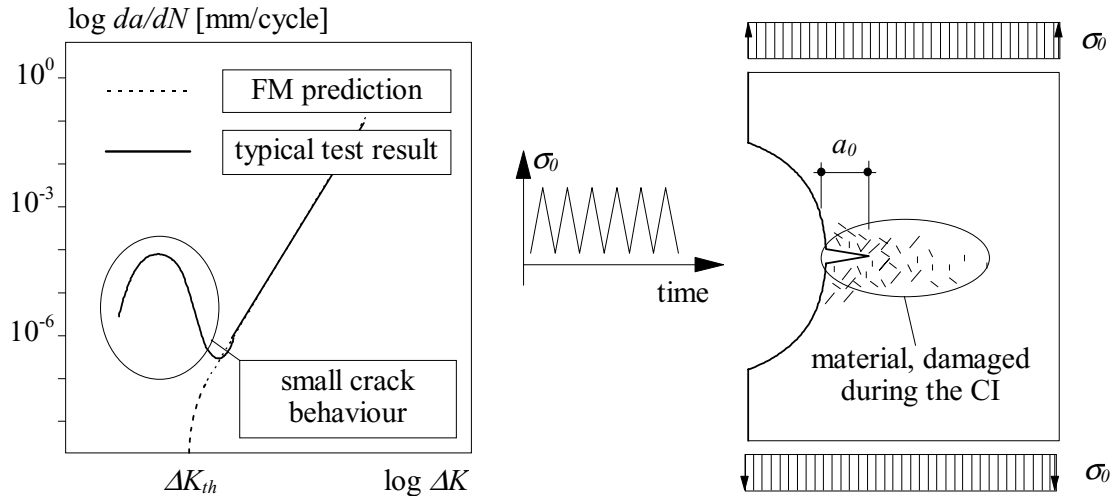


Figure 2.12 : Crack initiation induced damage - the explanation to small crack behavior.

Specimen thickness effect. The effect of specimen thickness is related to the stress-strain state at the crack tip region. The plastic zone at the crack tip due to plain stress is larger than the plastic zone due to a plain strain state. Consequently, the residual tensile deformations (plastic strip) and the opening stresses are also larger. A plane stress condition leads to smaller cyclic deformations at the crack tip and to slower local damaging than a plain strain state. Thus, crack propagation under a plain stress condition is slower than under plain strain conditions. The effect of the specimen thickness on fatigue behavior should be taken into account in fatigue crack propagation modeling.

Crack initiation and constraint under cyclic compression. Experiments have shown that the application of only compressive loads on a detail can cause the initiation of a fatigue crack, but further crack propagation will eventually cease [2.55]. The crack initiation occurs due to the high cyclic compressive deformations that occur around the crack initiator. The material near the crack initiator is subjected to non-linear cyclic strains which cause micro-crack nucleation and growth. This subsequently leads to the initiation of the fatigue crack (Figure 2.13.a).

Crack propagation will cease when the tip of the crack has grown out of the concentrated stress field around the crack initiator. If compressive loads are applied to a *cracked* detail, the fatigue crack itself is *not* the stress concentrator. This is because compressed cracks always remain closed and the flow of the compressive forces can be transferred not only by non-cracked material, but also through the contact surfaces of crack edges. This leads to a very small cyclic strain range in the region of the crack tip and does not cause noticeable damaging of the material. Thus, fatigue crack propagation stops (Figure 2.13.b).

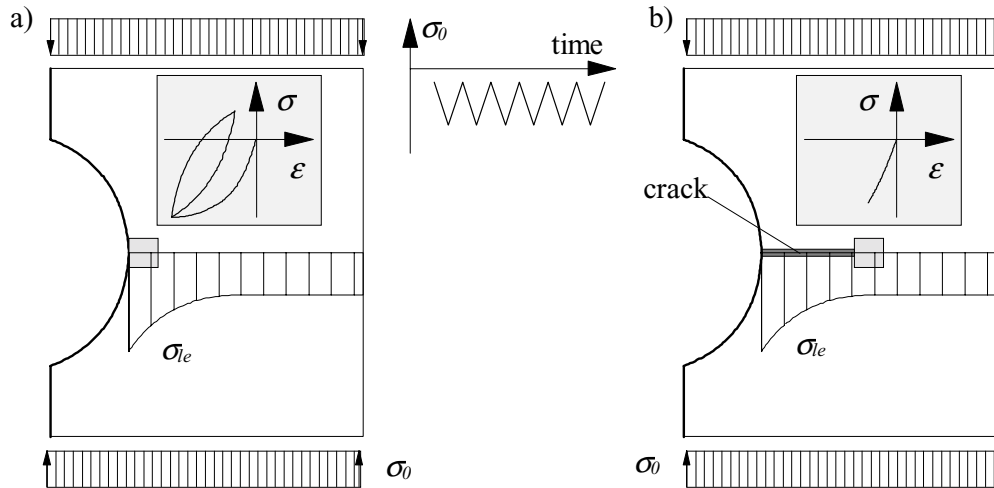


Figure 2.13 : Crack initiation (a) and arrest (b) due to cyclic compression.

2.3.4 Damage Accumulation

Before analyzing fatigue life prediction methods, the concept of damage accumulation will be introduced. Methods to estimate damage accumulation are required to account for the influence of variable-amplitude loading.

It was mentioned in Clause 2.3.2, that fatigue crack propagation occurs as a result of the gradual local *damaging* and failure of the material. *Local* damaging occurs as micro-crack nucleation and growth. This local damage turns into *global* damage as the micro-crack(s) join to form the fatigue crack and the fatigue crack advances. In summary, fatigue crack propagation can be thought of as the *damage accumulation* as function of load cycles from zero (no fatigue crack) to unity (detail failure).

Damage accumulation as function of load cycles can be graphically presented with a *relative* crack propagation curve. Tests show that the fatigue crack propagation curve (*a-N* curve) is non-linear, changing as function of loading, detail geometry, material properties, and fabrication-introduced residual stresses. The fact that the fatigue crack propagation curve is non-linear also implies that the fatigue damage accumulation can be regarded as a *non-linear* process.

From the practical point of view, it is inconvenient to deal with *non-linear* damage accumulation. Palmgren [2.35] and Miners [2.36] proposed the *linear* damage accumulation concept¹. This concept states that the damage caused to the detail by *one* load cycle at the load range *i*, is reciprocal to the fatigue resistance of the detail at the same load range, $N_{f,i}$:

$$d_i = \frac{1}{N_{f,i}} \quad (2.10)$$

The damage due to the n_i load cycles of the load range *i*, is :

$$d_{i,n} = n_i \cdot d_i = \frac{n_i}{N_{f,i}} \quad (2.11)$$

¹ The linear damage accumulation can be imaged like the water dropping into the bucket : if there is no water in the bucket - the damage is zero, and if the bucket is full - the damage is unity. The load cycles are the drops of variable volume, depending on the load range : higher cycles are bigger drops and lower cycles are smaller drops. The number of load cycles until failure is the amount of drops in full bucket.

and the total damage caused to the detail by the load cycles of different load levels is :

$$D_{tot} = \sum_i d_{i,n} = \sum_i \frac{n_i}{N_{f,i}} \quad (2.12)$$

Linear and non-linear damage accumulation curves are presented in Figure 2.14. It can be seen that generally there is a large difference between the linear and non-linear damage accumulation curves. The Palmgren-Miner's linear damage accumulation concept is a rough simplification of the physical damaging process.

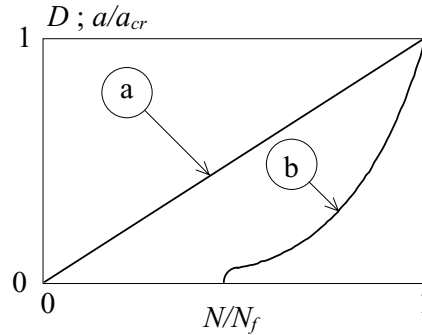


Figure 2.14 : Linear (a) and non-linear (b) damage accumulation.

2.4 FATIGUE LIFE PREDICTION METHODS

The ultimate aim of fatigue crack propagation modeling is to predict fatigue life of structural details. In this section, the common methods of fatigue life prediction are analyzed in order to compare the advantages and disadvantages of each method. This discussion is useful for the development of a new fatigue crack propagation model - the advantages of existing methods will be exploited while known disadvantages will be avoided.

	Fatigue life prediction method	LL-relationship	Parameter of the LL-relationship
1	<i>S - N curve</i> based approach	<i>S - N curve</i>	$\Delta\sigma_R$
2	local strain approach	strain-life relationship	$\Delta\varepsilon$
3	fracture mechanics approach	Paris equation	ΔK

Table 2.1 : Fatigue life prediction methods as a function of LL-relationship.

Each fatigue life prediction method is predicated on a relationship between some load related parameter and the fatigue life. This relationship can be called *load-life relationship* (LL-relationship). Briefly, a load-life relationship determines the relationship between some load related parameter and fatigue life of a detail of given material and geometry. The most common fatigue life prediction methods and the LL-relationships used by them, are presented in Table 2.1. In following three sections, these fatigue life prediction methods will be analyzed.

2.4.1 S-N Curve Based Approach

Load-Life Relationship

The load-life relationship used by the S - N curve based approach is an S - N curve having the following form :

$$\Delta\sigma_R = \text{Max} \left[\left(\frac{N_f}{C_1} \right)^{\frac{1}{-m_1}} ; \Delta\sigma_D \right] \quad (2.13)$$

where $\Delta\sigma_R$ is the load-related parameter of the load-life relationship. Sometimes the load-life relationship is given by three terms :

$$\Delta\sigma_R = \text{Max} \left[\left(\frac{N_f}{C_1} \right)^{\frac{1}{-m_1}} ; \left(\frac{N_f}{C_2} \right)^{\frac{1}{-m_2}} ; \Delta\sigma_{\text{CUT-OFF}} \right] \quad (2.14)$$

Equations (2.13) and (2.14) are called S - N curves (where S is the *Stress range* and N is the *Number of cycles*) or fatigue resistance curves (each S - N curve determines fatigue resistance of the specific detail). The constants C_1 , C_2 , m_1 and m_2 , as well as $\Delta\sigma_D$ and $\Delta\sigma_{\text{CUT-OFF}}$ in Equations (2.13) and (2.14), are determined using a *statistical analysis* of the constant-amplitude fatigue test results and depend essentially on the geometry of the test specimens. S - N curves have been introduced into the fatigue design codes [2.37], [2.38], [2.39], and the determination of the parameters in Equations (2.13) and (2.14) is relatively simple.

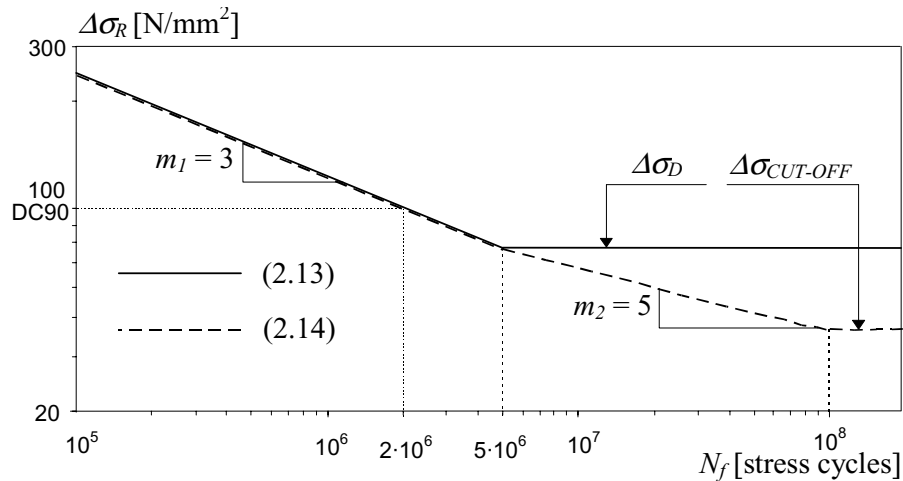


Figure 2.15 : S - N curves for DC90 [2.37].

Design codes classify fatigue resistance curves as functions of the detail geometry used in fatigue tests. Details with similar geometry are classified in the same group and form a *detail category* (DC). Two fatigue resistance curves for detail category 90 are presented in Figure 2.15.

Prediction of the Fatigue Life

The use of the S - N curve based approach in fatigue life predictions is relatively simple. If the constant amplitude loading is analyzed, then the fatigue life N_f can be calculated directly from Equations (2.13) or (2.14). If *variable-amplitude* loads are applied on the detail, then direct

calculation of the fatigue life is not possible. 3 steps are needed to carry out a fatigue analysis of a detail, loaded with variable-amplitude loads :

1. Arrange the applied load history in a load range histogram using some cycle counting method. Rainflow cycle counting method is preferred because it takes into account both visible and 'hidden' load cycles of the load history [2.2], [2.40] ;
2. Calculate the damage due to the entire load-range histogram, D_{tot} , using the linear damage accumulation rule (2.12). The N_{fi} in Equation (2.12) for each load range $\Delta\sigma_i$ in the load-range histogram, can be computed using Equations (2.13) or (2.14) ;
3. Calculate the fatigue life using Equation (2.15). Fatigue life by Equation (2.15) is calculated as the number of load range *histograms* and not in load *cycles*. One load range histogram can contain the cycles due to one train pass over the bridge, for example. In that case, the fatigue life appears in train passages.

$$N_f = \frac{I}{D_{tot}} \text{ [load range histograms]} \quad (2.15)$$

The $S-N$ curves based approach takes into account the *fatigue threshold*. The fatigue threshold is assumed to be reached if the nominal stress range is less than the constant-amplitude fatigue limit : $\Delta\sigma_R < \Delta\sigma_D$ (if Equation (2.13) is used); or if the nominal stress range is less than the cut-off limit : $\Delta\sigma_R < \Delta\sigma_{CUT-OFF}$ (if Equation (2.14) is used).

Unfortunately, the fatigue life predictions using the $S-N$ curves, often result in conservative and uncertain results. The conservatism of the results occurs mainly due to the safety factors included into the constants of the $S-N$ curves. The uncertainty of the results is mainly due to the uncertainties in the *linear* damage accumulation concept. Consequently, the $S-N$ curves should be used for fatigue design and *not* for evaluation of remaining fatigue life.

The *advantages* of the $S-N$ curve based approach are :

- it is relatively simple to use ;
- it is safe to use ; because it is based on a great amount of fatigue test results;
- it takes into account the fatigue threshold.

The *disadvantages* of the $S-N$ curve based approach are :

- little precision and over-conservatism in fatigue life predictions, especially in the region where $\Delta\sigma_R$ is low and when variable-amplitude loading is considered ;
- an $S-N$ curve based approach does not distinguish between steel grades : all structural steels are assumed to have a similar fatigue behavior ;
- an $S-N$ curve based approach does not directly quantitatively take into account the influence of various aspects of fatigue crack propagation, such as crack closure effect, thickness effect, small crack behavior, etc..

2.4.2 Local Strain Approach

Load-Life Relationship

The load-life relationship used by the local strain approach is :

$$\frac{\Delta\varepsilon}{2} = \frac{\sigma_f - \sigma_m}{E} \cdot (2 \cdot N_f)^{b'} + \varepsilon_f \cdot (2 \cdot N_f)^{c'} \quad (2.16)$$

where the load-related parameter of the load-life relationship is the strain *range*, $\Delta\varepsilon$. Equation (2.16) is called a *strain-life relationship*. The strain *amplitude* $\Delta\varepsilon/2$ in the Equation (2.16) can be written as the sum of the elastic strain amplitude $\Delta\varepsilon_e/2$ and the plastic strain amplitude $\Delta\varepsilon_{pl}/2$:

$$\frac{\Delta \varepsilon}{2} = \frac{\Delta \varepsilon_{el}}{2} + \frac{\Delta \varepsilon_{pl}}{2} \quad (2.17)$$

where

$$\frac{\Delta \varepsilon_{el}}{2} = \frac{\sigma'_f - \sigma_m}{E} \cdot (2 \cdot N_f)^{b'} \quad (2.18)$$

and

$$\frac{\Delta \varepsilon_{pl}}{2} = \varepsilon'_f \cdot (2 \cdot N_f)^{c'} \quad (2.19)$$

Equation (2.18) and Equation (2.19) are the elastic and plastic components of the strain-life relationship (2.16). All three equations are graphically presented in Figure 2.16.

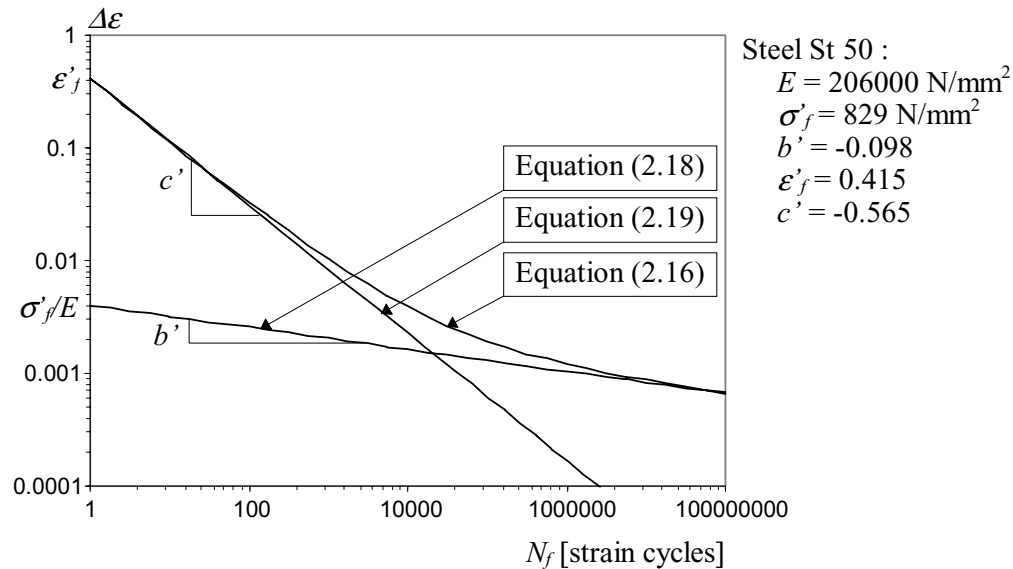


Figure 2.16 : Strain-life equations for steel St50 [2.47].

Equation (2.18) was first introduced by Basquin [2.41]. In order to consider the effect of the mean stress, σ_m , the Equation (2.18) was modified by Morrow [2.42]. Equation (2.19) was proposed by Coffin [2.43] and Manson [2.44] who worked independently on thermal fatigue problems. In the literature, Equation (2.19) is known as the Coffin-Manson equation.

The strain-life relationship (2.16) contains 5 material-dependent constants : E , σ'_f , b' , ε'_f , c' . Methods to determine of these constants are standardized [2.45], [2.46], and handbooks containing these constants for various materials have been published [2.47]. Fatigue properties of the material are determined by the constants σ'_f , b' , ε'_f , c' . The values of these constants strongly depend on the steel grade or the aluminum alloy used, and on the fabrication method of the rough material.

In addition to the experimental determination of the constants used in the strain-life relationship, several empirical relationships exist in order to calculate them. Morrow [2.42] developed the relationships between constants b' and c' and the material cyclic strain hardening exponent n' :

$$b' = \frac{-n'}{1 + 5 \cdot n'} \quad (2.20)$$

and

$$c' = \frac{-1}{1 + 5 \cdot n'} \quad (2.21)$$

Like Morrow [2.42], but using a different method, Krajcinovic and Lemaitre [2.3] found a relationship between material cyclic stress-strain parameters¹ and constants b' and c' . Herzberg [2.27] has remarked that the cyclic strength coefficient, σ_f' , is approximately equal to the monotonic fracture strength :

$$\sigma_f' \approx \sigma_f \quad (2.22)$$

The fatigue ductility coefficient is about 30% to 100% of the monotonic fracture ductility :

$$\varepsilon_f' = 0.3 \text{ to } 1.0 \cdot \varepsilon_f \quad (2.23)$$

Herzberg [2.27], comparing the strain-life relationships of strong, tough, and ductile alloys, observed that ductile alloys perform better under high cyclic strains than strong alloys. However, strong alloys are superior when low strains are applied (Figure 2.17).

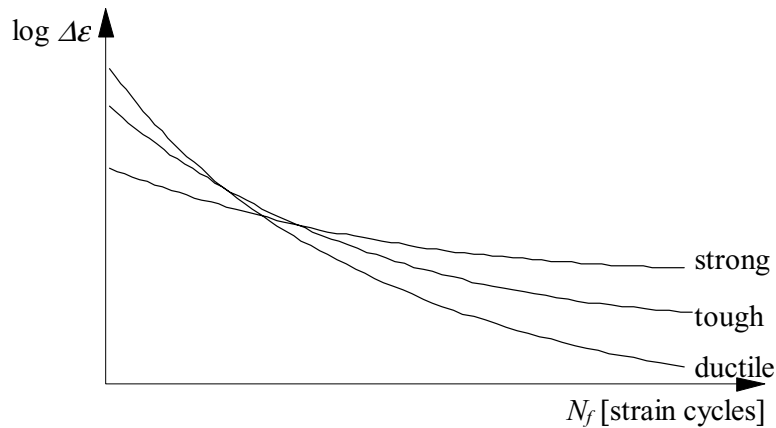


Figure 2.17 : Schema showing the optimum material for a given total strain amplitude [2.27].

Prediction of the Fatigue Life

Unfortunately, the local strain approach can only be used for the prediction of the *crack initiation* period : calculation of the $\Delta\varepsilon$ at the crack initiator is relatively simple, and if $\Delta\varepsilon$ is known, using Equation (2.16) and iteration, one can determine the crack initiation period. On the other hand, calculation of the $\Delta\varepsilon$ at the fatigue crack tip is more complex. This is because the cyclic strain field at the crack tip changes all the time due to crack growth, and consequently, calculation of the stable growth period using Equation (2.16) is impossible.

The strain range $\Delta\varepsilon$, occurring near the crack initiator usually contains both elastic and plastic terms and an exact value is very difficult to calculate. However, the strain range $\Delta\varepsilon$ at the crack initiator can be computed using approximate methods. A widely used approximate

¹ The cyclic stress-strain parameters (the strain hardening exponent n' , and the cyclic strength coefficient K') are more closely reviewed in Chapter 3.

method is Neuber's rule [2.48]. Neuber's rule enables one to calculate the *elastic-plastic* strain range using the *linear-elastic* stress range. The alternative calculation method of the elastic-plastic strain range - Glinka's equivalent strain energy density criterion (ESED criterion), is explained in Clause 3.3.4.

In the local strain approach, the crack initiation period due to variable-amplitude loading can be calculated. Similar to the *S-N* curve based approach, 3 calculation steps are required :

1. Arrange the applied load history in a load range histogram using some cycle counting method, and express the load histogram in terms of the local strain ranges in order to determine the strain range histogram ;
2. Calculate the damage due to the entire strain range histogram, D_{tot} , using the linear damage accumulation rule Equation (2.12), where the $N_{f,i}$ in Equation (2.12) for each strain range $\Delta\epsilon_i$ in the strain range histogram, can be computed using Equation (2.16) ;
3. Calculate the fatigue life using Equation (2.15).

The local strain approach does not consider the *fatigue threshold*. However, from an engineering point of view, the fatigue threshold is reached if the strain range leads to a fatigue life greater than 10^8 to 10^9 loading cycles.

The *advantages* of the local strain approach are :

- relatively high accuracy in crack initiation prediction ;
- the influence of material properties on the fatigue behavior accurately taken into account in this approach ;
- the influence of the local mean stress, σ_m , is taken into account ;
- the material cyclic stress-strain and fatigue parameters can be easily found in the literature or by using Equations (2.20), (2.21), (2.22) and (2.23).

The *disadvantages* of the local strain approach are :

- it can only be used to the predict the crack initiation period ;
- the constants of the strain-life relationship have to be known in order to apply this approach. To estimate these constants with testing is relatively time consuming.

2.4.3 The Fracture Mechanics Approach

Load-Life Relationship

The load-life relationship used by the fracture mechanics approach, is :

$$N_f = \int_{a_0}^{a_{cr}} \frac{1}{C \cdot \Delta K^m} \cdot da \quad (2.24)$$

where the load-related parameter of this relationship is the stress intensity factor range, ΔK . The denominator of Equation (2.24) comes from an empirical relationship, called the Paris equation [2.49] :

$$\frac{da}{dN} = C \cdot \Delta K^m \quad (2.25)$$

The prediction of the fatigue life is very dependent on the exponent m and constant C in Equation (2.25) and both constants are material dependent. Generally, m is taken 3 for structural steels. Many analytically derived relationships have been established between da/dN and ΔK . It is possible to relate the crack propagation rate, da/dN , to the crack tip opening displacement, *CTOD* [2.50]. The relationships between *CTOD* and da/dN lead to an exponent $m = 2$. However, using energy equilibrium conditions and thermodynamics of cracked bodies in order to relate da/dN and ΔK , an exponent of $m = 4$ is calculated [2.51], [2.52], [2.53]. Nevertheless, theoretical interpretations of Paris' equation fix the limits for the exponent m :

$2 \leq m \leq 4$. Glinka in [2.54] has derived m as a function of the fatigue ductility exponent, c' , and the cyclic strain hardening exponent, n' :

$$m = -\frac{2}{c' \cdot (n' + 1)} \quad (2.26)$$

The Paris equation constant C can be estimated using a measured crack propagation curve. Since fatigue crack propagation measurement requires precise equipment, the determination of the constant C is usually empirical and relatively complicated. Besides empirical determination of C , Glinka [2.54], using continuum mechanics and fatigue damage accumulation theory, has made an elegant theoretical attempt to relate C to the strain-life relationship constants. Further discussion of the determination of the constants C and m is made in Chapter 6.

Prediction of the Fatigue Life

The stress intensity factor ΔK applies if the crack length is greater than zero. Thus, the fracture mechanics approach can only be applied to the calculation of the stable crack growth period. The prediction of the stable crack growth period can be made using Equation (2.24). In most cases, ΔK is a complicated function of the crack length and shape and the detail geometry. Therefore, the integration of Equation (2.24) must be performed numerically.

Many modifications have been introduced into the Paris equation. These modifications account for the influence of various aspects of fatigue crack propagation. One of the most popular modifications to the Paris law accounts for the *fatigue threshold* (Equation 2.27). The threshold stress intensity factor range, ΔK_{th} , in Equation (2.27) can be determined from fatigue tests. From an engineering point of view, the fatigue threshold is reached if the *average* crack propagation rate is below $da/dN < 10^{-8}$ to 10^{-7} mm/cycle. Experiments have shown that ΔK_{th} depends on the minimum and maximum nominal load ratio R and on fabrication-induced residual stresses.

$$\frac{da}{dN} = C \cdot (\Delta K^m - \Delta K_{th}^m) \quad (2.27)$$

In the fracture mechanics approach, the stable crack growth under *constant-amplitude* and *variable-amplitude* loading can be calculated. For variable-amplitude fatigue behavior, the *crack closure effect* should be considered and the *effective* stress intensity factor range, ΔK_{eff} , has to be used in the Paris equation instead of ΔK .

The effective stress intensity factor can be calculated as function of the loading history and the crack geometry. There are many models available in the literature, which are capable of calculating the effective stress intensity factor. These models are generally called crack closure models and can be classified into 3 groups : *geometrical* models (dealing with the geometrical analysis of the crack edge plastic strip and the crack tip plastic zone [2.58], [2.55]) ; *empirical* models (the effective stress range or the effective stress intensity range are evaluated using empirical formulas [2.20], [2.56]) ; and *crack tip stress based* models (models which evaluate the effective stress intensity range from the residual stress field introduced at the crack tip region during unloading [2.21], [2.55]).

The *advantages* of the fracture mechanics approach are :

- the stress intensity factor concept can be used to predict the behavior of great variety of fatigue cracks using only one theory ;
- relatively high accuracy in fatigue failure prediction.

The *disadvantages* of the fracture mechanics approach are :

- the fracture mechanics approach can only predict the stable crack growth period;
- the determination of the stress intensity factor range and the integration of the Paris law is relatively complicated ;

- fatigue life prediction results are rather sensitive to the variation of the Paris law constant C and exponent n ; the determination of the parameters C and m is relatively complicated.

2.4.4 Dugdale Crack - Simple Crack Model

The Dugdale crack model will be discussed in this section. This model offers a method to analyze the dynamic behavior of fatigue crack using relatively simple formulas and it considers plate thickness effect (see Clause 2.3.3). The analysis of crack dynamics (closure and opening) makes it possible to model the crack closure effect thereby by accounting for the influence of the variable-amplitude loading on the fatigue crack propagation. The aim of this section is to present the formulas used to calculate the crack opening profile of the Dugdale crack for *any* loading event.

The Dugdale crack is the most commonly applied crack model. It was introduced by Dugdale [2.7] and is slightly different from the Barrenblatt crack model [2.8]. The Dugdale crack is introduced in a thin elastic plate of infinite length and width. Dugdale crack behavior is calculated using the basic theory of a crack in a linear-elastic body. However, the crack differs from the linear crack because a strip of elastically-perfect plastic material is added between the crack edges in the region of the tip. This added material simulates the effect of the crack tip plastic zone. In other words, the difference between the linear-elastic crack and the Dugdale crack is that the latter has the plastic zone and the former does not.

The Dugdale crack model assumes an effective crack which is longer than the physical crack (Figure 2.18). The crack edges, r_{pl} , in front of the physical crack carry the cyclic yield stress tending to close the crack. (The length r_{pl} is not cracked in reality, i.e., the material can still bear the yield stress). The size of r_{pl} is chosen such that the stress singularity at the tip of the Dugdale crack disappears, K should be zero. This means that the stress intensity $K(\sigma_0)$ due to the nominal stress σ_0 must be compensated by the stress intensity $K(\sigma'_{ys})$ due to the wedge forces σ'_{ys} :

$$K(\sigma_0) + K(\sigma'_{ys}) = 0 \quad (2.28)$$

Plastic Constraint Factor

The plate thickness has an influence on a stress-strain state at the crack tip, and therefore, on the crack propagation. At the tip of the crack in *thin* plate, plain stress conditions prevail. At the tip of the crack in *thick* plate, plain strain conditions prevail. In order to account for the influence of the plate thickness, Broek [2.14] introduced a plastic constraint factor. The plastic constraint factor, pcf , is the ratio of the maximum stress to the cyclic yield stress. The quantity $pcf \cdot \sigma'_{ys}$ can be called an effective cyclic yield stress. Using the Von Mises yield criterion, Broek proposes:

$$pcf = 3 \quad (2.29)$$

in the presence of plain strain (thick plate), and:

$$pcf = 1 \quad (2.30)$$

in the presence of plain stress (thin plate). Depending on the thickness of the cracked plate or the location of the crack tip in the detail¹, $1 \leq pcf \leq 3$. (Irwin [2.57], for example, takes $pcf = 1.68$.)

¹ At the plate surface, the plain stress state always prevails.

Dugdale Crack at $\sigma_{0,max}$

The plastic zone resists the opening of a loaded Dugdale crack. The resistance of the plastic zone to the opening of the crack can be replaced by the effective cyclic yield stress $pcf \cdot \sigma'_{ys}$, acting on the crack edges along the length r_{pl} (Figure 2.18).

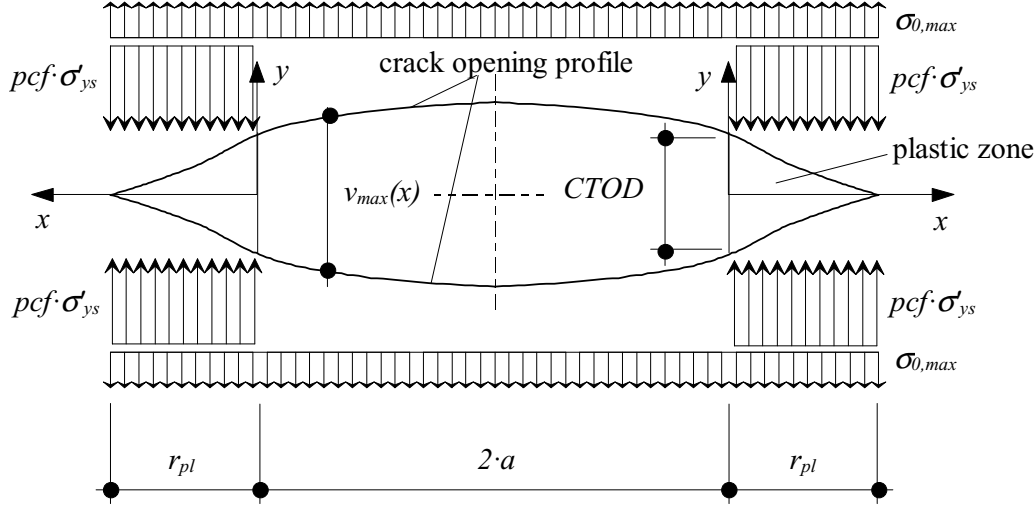


Figure 2.18 : Dugdale crack at $\sigma_{0,max}$.

The plastic zone size, r_{pl} , can be found from (2.28). It results in an equation which contains many terms. Neglecting the higher order terms results in Equation (2.31) [2.14].

$$r_{pl} = \frac{\pi}{8} \cdot \left(\frac{K}{pcf \cdot \sigma'_{ys}} \right)^2 \quad (2.31)$$

The crack tip opening displacement of a loaded Dugdale crack can be calculated using the Equation (2.32) [2.14].

$$CTOD = \frac{4}{\pi} \cdot \frac{K^2}{pcf \cdot \sigma'_{ys} \cdot E} \quad (2.32)$$

The crack opening profile of a loaded Dugdale crack, at any coordinate of its edge, is related to the $CTOD$ and r_{pl} as follows :

$$v_{max}(x) = CTOD \cdot g\left(\frac{x}{r_{pl}}\right) \quad (2.33)$$

where $g(\xi)$ is the unit crack opening profile function [2.5] and $x=-a$ to r_{pl} . The function $g(\xi)$ can be calculated using Equation (2.34) :

$$g(\xi) = \sqrt{1-\xi} - \frac{\xi}{2} \cdot \ln \left| \frac{1+\sqrt{1-\xi}}{1-\sqrt{1-\xi}} \right| \quad (2.34)$$

Dugdale Crack at $\sigma_{0,min}$

When unloading the Dugdale crack, the elastic material around it attempts to return to its initial position. This is not possible because the elastic energy, contained in the loaded plate,

is not sufficient enough to force the plastic zone created during loading, to disappear. A small portion of the plastic zone will, however, undergo *cyclic* plastic deformations. This re-deformed part of the plastic zone is called a *cyclic plastic zone*.

It can be assumed that during cyclic compression, a plain stress state always prevails at the crack tip [2.14]. Therefore, the plastic constraint factor is 1 during compression, $pcf = 1$ and the effective cyclic yield stress range is $(pcf+1) \cdot \sigma'_{ys}$ (Figure 2.19). In calculations, the influence of plastic zone on an *unloaded* Dugdale crack can be replaced by the effective cyclic yield stress range (Figure 2.20).

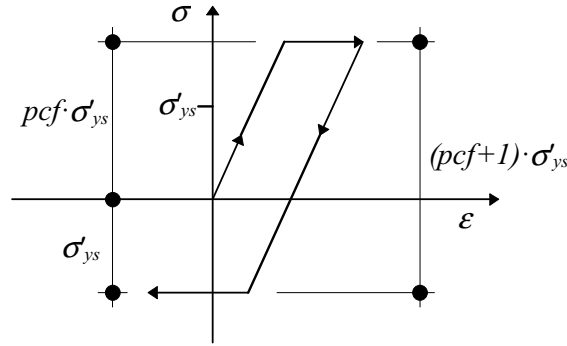


Figure 2.19 : Effective cyclic yield stress and effective cyclic yield stress range.

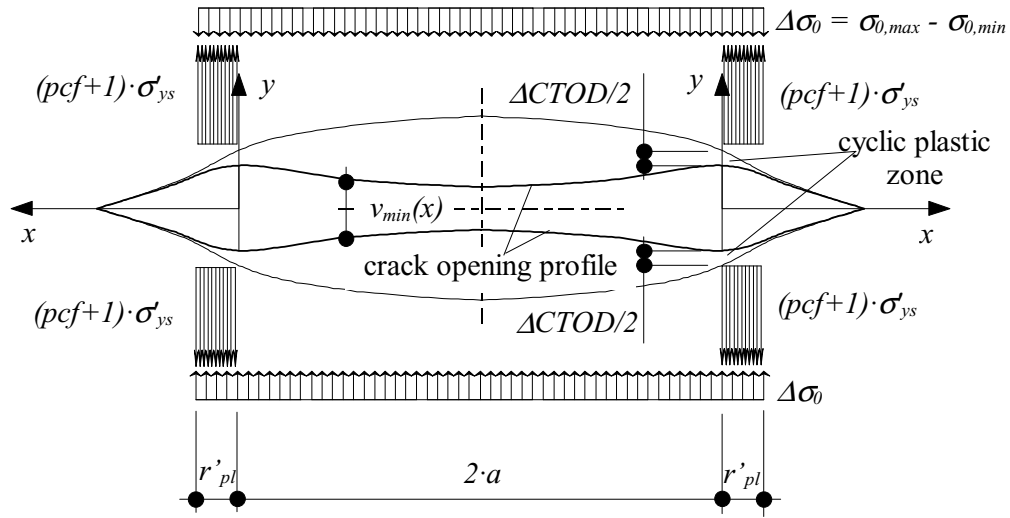


Figure 2.20 : Dugdale crack at $\sigma_{0,min}$.

The size of the cyclic plastic zone, r'_{pl} , can be calculated by substituting the stress intensity factor range ΔK and the effective cyclic yield stress range, $(pcf+1) \cdot \sigma'_{ys}$, for the K and $pcf \cdot \sigma'_{ys}$ into Equation (2.31) :

$$r'_{pl} = \frac{\pi}{8} \cdot \left(\frac{\Delta K}{(pcf+1) \cdot \sigma'_{ys}} \right)^2 \quad (2.35)$$

where

$$\Delta K = K_{max} - K_{min} \quad (2.36)$$

The cyclic crack tip opening displacement $CTOD'$ can be calculated by substituting the stress intensity factor range, ΔK , and the effective cyclic yield stress range, $(pcf+1) \cdot \sigma'_{ys}$, for K and $pcf \cdot \sigma'_{ys}$ into Equation (2.32) :

$$CTOD' = \frac{4}{\pi} \cdot \frac{\Delta K^2}{(pcf + 1) \cdot \sigma'_{ys} \cdot E} \quad (2.37)$$

The crack opening profile of an *unloaded* Dugdale crack at any coordinates at the edge, is related to the v_{max} , $CTOD'$ and r'_{pl} as follows :

$$v_{min}(x) = v_{max}(x) - CTOD' \cdot g\left(\frac{x}{r'_{pl}}\right) \quad (2.38)$$

where v_{max} , $CTOD'$, $g(\xi)$ and r'_{pl} can be calculated using Equations (2.33), (2.37), (2.34) and (2.35) reciprocally.

Suresh in [2.5], referring to the work of Budiansky and Hutchinson [2.58], presents an equation, similar to Equation (2.38), for the loading case where $\sigma_{0,min}=0$ only. Here Equation (2.38) is a generalization of the function, proposed by Budiansky and Hutchinson [2.58]. The crack opening profile function of an the Dugdale crack at $\sigma_{0,min}$ (Equation 2.38), is valid only if there is *no* contact between the crack edges.

2.5 SUMMARY AND CONCLUSIONS

Stress concentrators

Fatigue occurs close to stress concentrators, which are geometrical irregularities in the detail. Stress concentrators can be divided into two groups : crack initiators (notches, welds, holes, etc.) and fatigue cracks. Fatigue cracks initiate at the crack initiators and grow along a path perpendicular to the highest principal stresses in the stress field around the crack initiator. The location of the crack initiation and the crack growth path can be determined from analysis of the detail geometry.

If a detail is loaded, a concentrated stress field occurs around the stress concentrators. The stress field around the crack initiator can be calculated using the stress concentration factor. The stress field around the fatigue crack can be calculated using the stress intensity factor. The influence of fabrication-induced residual stresses on the stress field can also expressed using the stress concentration factor and the stress intensity factor.

Fatigue crack propagation

Fatigue crack propagation can be divided into three stages : crack initiation, stable crack growth, and unstable crack growth. The first two stages constitute the primary portion of the fatigue life and both must be included in modeling. The third stage is very short and therefore unimportant from a modeling point of view.

The crack initiation stage and the primary portion of the stable crack growth stage takes place as a result of perpetual nucleation and growth of the micro-cracks near the stress concentrators. Since the physical mechanisms of crack initiation and stable crack growth are the same, these stages should be modeled according to the same principles. At the end of the stable crack growth stage and during the unstable crack growth stage, fatigue crack growth occurs as a result of local fracture of the material.

A fatigue crack propagation model should be able to take into account various aspects of fatigue crack propagation, such as fatigue threshold, crack closure effect, load effects, plate

thickness effect, small crack behavior, and crack initiation and arrest under cyclic compression.

Fatigue crack propagation can also be regarded as *nonlinear* damage accumulation process. In calculations, a *linear* damage accumulation concept is often used. However, the use of a linear damage accumulation concept instead of a nonlinear approach, leads to large uncertainties in the results. This uncertainty is even larger if variable-amplitude fatigue behavior is analyzed.

Fatigue life prediction methods

Three common fatigue life prediction methods exist : $S-N$ curve based approach, local strain approach, and fracture mechanics approach. Each uses a different load-life relationship (i.e. a relationship between some load-related parameter and fatigue life). The advantages and disadvantages of these methods depend on the simplicity of use, the accuracy of the prediction, and on the scope of the application range.

The $S-N$ curve based approach is simple to use, but the results in fatigue life predictions that are not accurate. The local strain approach is accurate enough and the range of application is wide. However, it can only be applied to the prediction of the crack initiation period. Fatigue life predictions using the fracture mechanics approach are more accurate, but the method can only be applied on the calculation of the stable crack growth period.

In order to analyze variable-amplitude fatigue behavior, the crack closure effect must be considered. The crack closure effect is related to the dynamic behavior of the crack. The Dugdale crack is a simple crack model that in a relatively facile way can be used to analyze the opening and closure of a cyclically loaded crack. The Dugdale crack can therefore be used as the basis of the crack closure model.